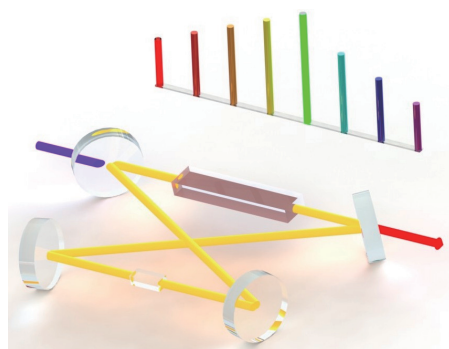


ARTICLE

Frequency-Stabilized Mid-infrared Laser Source for Precision Spectroscopy[†]Yan-Dong Tan^{a,b,‡}, Jinjin Chen^{a,‡}, Yong Zhou^{a*}, Cun-Feng Cheng^{b*}, Shui-Ming Hu^{b,c*}*a. Anhui Province Key Laboratory for Control and Applications of Optoelectronic Information Materials, Department of Physics, Anhui Normal University, Wuhu 241000, China**b. Department of Chemical Physics, University of Science and Technology of China, Hefei 230026, China**c. State Key Laboratory of Molecular Reaction Dynamics, University of Science and Technology of China, Hefei 230026, China*

(Dated: Received on January 1, 2024; Accepted on January 26, 2024)

Precision measurements on molecules in the strong fundamental bands are of great importance. An accurate mid-infrared light source is a key for these studies. By locking the signal and pump light to an optical frequency comb, a high-precision continuous-wave optical parametric oscillator source is built, and the mid-infrared frequency drift is determined to be less than 1 kHz. As a demonstration, saturated absorption spectroscopy of the R(14)(00011)–(00001) line of $^{13}\text{CO}_2$ is measured, and the transition frequency is determined to be 68786813496(29) kHz. The frequency-stabilized mid-infrared laser source provides an opportunity for precision measurements of molecules in fundamental bands.

**Key words:** Mid-infrared, Accurate laser source, Precision spectroscopy

I. INTRODUCTION

With the development of laser techniques, spectroscopic methods have been employed in precision measurements to test fundamental physics and search for new physics [1, 2]. The development of high-precision spectroscopy methods makes it possible for an accurate read-out of the transition frequency as the good examples in optical clocks [3, 4], leading to notable achievements in the application in atomic systems [5–8]. Precision measurements in molecular systems in the last two decades have been used to test quantum electrodynamics (QED) theory and determine fundamental con-

stants [9–11], probe the variation of the constant values [12–14], study the intramolecular parity-violation effects [15], and search for the possible existence of new physics beyond the standard model [16, 17].

Novel high-resolution and highly-sensitive spectroscopy techniques have been employed in the precision measurements on molecules for the studies of fundamental physics [2, 9, 18, 19], as well as the rapid and accurate analysis of trace gases [20–22]. Fundamental vibrational bands of molecules, usually one or two orders of magnitude stronger than the overtone bands, are considered more likely to achieve high precision. Because the fundamental vibrational bands are in the mid-infrared (MIR) wavelength region, high-sensitivity MIR spectroscopy methods enable a better analysis of molecules in various processes involving the fields of physics, chemistry, atmosphere, and bioscience. The development in sensitivity of MIR spectroscopy can be combined with other techniques, such as supersonic molecular beam and velocity map imaging, which are possibly useful for precision measurements and chemi-

[†] Part of Special Issue “In Memory of Prof. Qihe Zhu on the occasion of his 100th Anniversary”.

[‡] These authors contributed equally to this work.

* Authors to whom correspondence should be addressed. E-mail: yong.zhou@mail.ahnu.edu.cn, cfcheng@ustc.edu.cn, smhu@ustc.edu.cn

cal dynamics research.

Although there are application requirements, compared with advanced visible and near-infrared (NIR) laser spectroscopy systems, MIR precision spectroscopy has some inconveniences regarding the laser source and frequency calibration. Numerous MIR laser sources have been reported in the past few decades. The gas lasers have high output power and narrow linewidth, leading to a broad application in precision spectroscopy measurements [23, 24]. However, limited by the species of the gain medium, the gas laser only works around a few wavelengths. The development of quantum well engineering technology makes the commercial quantum cascade lasers (QCLs) [25, 26] the most widely used laser source in the MIR. But the laser linewidth is usually in the 2–10 MHz range, and the frequency calibration needs MIR frequency reference such as MIR combs [27] that are not yet refined, or up-conversion to an accessible wavelength region, which may introduce complexity. Utilizing the nonlinear effect is an alternative way to generate MIR laser emission. Based on the advanced periodically poled lithium niobate (PPLN) crystal the differential frequency generation [28, 29] and high-efficiency continuous-wave optical parametric oscillator (OPO) [30–32] are the widespread techniques, which have broad tuning range and can be calibrated by NIR frequency references. Even so, achieving sufficient laser power and accurate frequency remains a big challenge.

In this work, we report an accurate OPO system with the MIR frequency stabilized by a NIR comb. As a demonstration, the sub-Doppler saturated absorption spectroscopy of the rovibrational transition of $^{13}\text{CO}_2$ at 4.3 μm is recorded, and the transition frequency is determined with high precision.

II. METHOD

The experimental scheme is illustrated in FIG. 1. The setup comprises two main components: a frequency-stabilized MIR laser source and a saturated absorption spectrometer. The frequency-stabilized MIR laser source is based on a home-made OPO and frequency locking system. The OPO is pumped by a 1064 nm narrow-linewidth Nd:YAG laser with a maximum output power of 15 W. The pump laser delivers the laser beam to a PPLN crystal, which is designed to be a multi-channel type 5% MgO doped PPLN crystal with an effective length of 5 cm. The NIR signal light is generated through the non-linear effect of the PPLN, and the

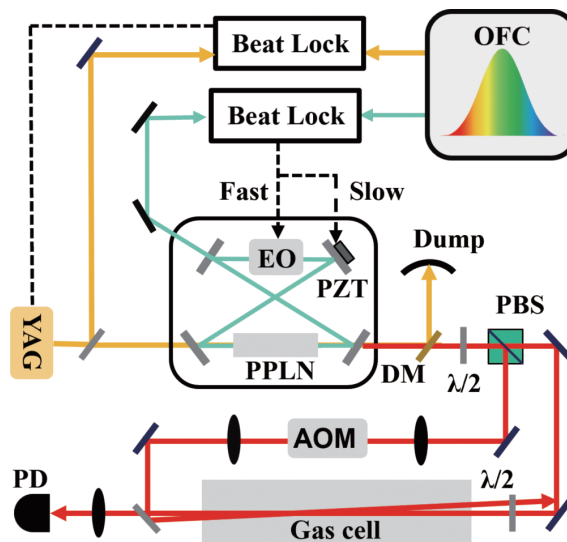


FIG. 1 Schematic of the spectroscopy setup. The orange, green, and red lines represent the pump, signal, and idler light beams of the OPO light source, respectively. Abbreviations: YAG: Nd:YAG laser; PPLN: periodically poled lithium niobate; EO: electro-optical crystal; AOM: acousto-optical modulator; PD: photodiode detector; OFC: Optical frequency comb; PZT: piezoelectric actuator; DM: dichroic mirror; PBS: polarized beamsplitter; $\lambda/2$: half waveplate.

power is enhanced by a bow-tie ring cavity. The mid-infrared idler light is then generated when the pump laser power reaches the lasing threshold. The idler light output has a power of up to hundreds of milliwatts at around 4.3 μm after good phase matching. The PPLN crystal is installed in the oven inside the ring cavity, allowing precise temperature control ranging from 300 K to 450 K with the stability of 2×10^{-3} K, as well as precise position control with a position resolution of 10 μm . The ring cavity consists of four highly reflective mirrors with a reflectivity of approximately 99.9% for the signal light and less than 0.5% for both pump and idler lights. Because the frequency of the idler light is equal to the frequency difference between the pump and signal light due to the law of energy conservation, the MIR idler light frequency can be stabilized if both the pump and signal light frequencies are well-locked.

Using a beat-lock servo [33] we are able to lock the pump and signal light to the NIR optical frequency comb (OFC). Meanwhile, the absolute frequency of the MIR laser is known by monitoring the pump and signal light frequencies at the same time by the OFC. The pump light, the linewidth of which is guaranteed by the company to be less than 5 kHz in 10 ms integration time, has to be locked to the OFC to reduce the long-term frequency drift. A home-made beat-lock circuit is

used to transfer the beat signal between the pump light and the OFC mode to an error signal, and slow feedback with a bandwidth of 10 Hz is sent to the piezoelectric actuator (PZT) to tune the pump light frequency. The short-term frequency fluctuation of the signal light comes from the pump light linewidth and the additional vibrational noise of the ring cavity, and the long-term frequency drift is due to the optical path drift of the ring cavity. To lock the signal light frequency, an electro-optic (EO) crystal is placed inside the ring cavity. The refractive index of the crystal is controlled by a feedback servo by applying an external electric field, and the fast frequency fluctuation of the signal light can be compensated. A PZT is attached to one of the cavity mirrors to compensate for the slow optical length changes [34]. The error signal is generated from the beat signal between the signal light and the OFC mode, and the fast and slow feedbacks with corresponding bandwidths of 3 MHz and 10 Hz, limited by the feedback loop, are applied to the EO and PZT, respectively. When both the pump and signal lights are locked, the frequency of the idler light is stabilized. With the method mentioned above, the short-term stability is as good as the pump light, and the long-term stability is as good as the OFC mode.

The MIR idler light is then split into two beams, serving as the pump laser and probe laser in the saturated absorption spectroscopy scheme, as shown in FIG. 1. The pump laser beam is frequency shifted by +80 MHz using an acousto-optic modulator (AOM). Consequently, the center of the Lamb-dip signal is blue-detuned by 40 MHz relative to the transition center frequency.

Fine tuning of the MIR light can be accomplished by adjusting the beat-lock reference frequency of either the pump or the signal light. This tuning method maintains kilohertz or even better accuracy at each frequency point and has a tuning range of about 100 MHz, which is limited by the beating electronics and the repetition frequency of the OFC. Coarse tuning of the MIR light is achieved by changing the PPLN temperature from 300 K to 450 K, which allows for a tuning range of more than 80 cm^{-1} with a PPLN period of $27.6667 \text{ }\mu\text{m}$.

III. RESULTS AND DISCUSSION

The frequency of the MIR laser output is determined by measuring the frequencies of the pump and

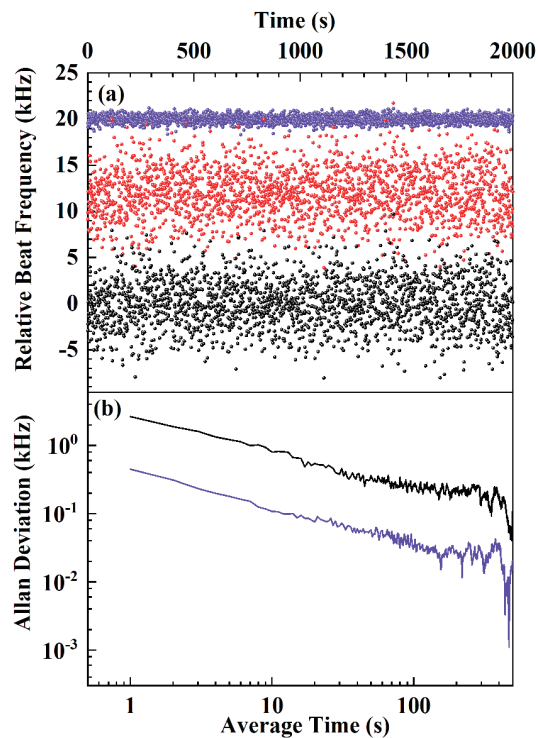


FIG. 2 Frequency drift of the frequency-stabilized laser. (a) Beat frequency between the pump (signal) laser of OPO and the comb. Purple and red color represent the pump and signal lasers, respectively. The black data points represent the difference between the pump and signal laser, indicating the frequency of the idler laser. Data are shifted for better illustration. (b) Allan deviation of the pump, signal, and idler light frequencies given in (a). The frequency fluctuation of the idler light is dominated by that of the signal light, therefore their Allan deviation curves are overlapped.

signal lights of the OPO source. To evaluate the frequency accuracy, we first monitored the beat frequency between the pump (probe) laser and the NIR OFC mode. The carrier-envelope offset frequency and the repetition frequency of the comb are phase-locked to a hydrogen maser with a fractional frequency uncertainty better than 1×10^{-13} . Thus, the absolute frequency of each comb mode is as accurate as 13 digits, resulting in an excellent frequency reference for laser frequency locking and monitoring. The frequency monitoring results are shown in FIG. 2(a), and the Allan deviations are shown in FIG. 2(b). Note that the MIR laser frequency, derived by the difference between the measured frequencies of the pump and signal lights, fluctuates at about 0.1 kHz after an average time of 300 s. The result agrees well with our previous study [34]. The measured frequency drift under 10 s averaging time is less than 1 kHz, and the frequency uncertainty of the laser is better than 0.6 kHz during a spectroscopy scan

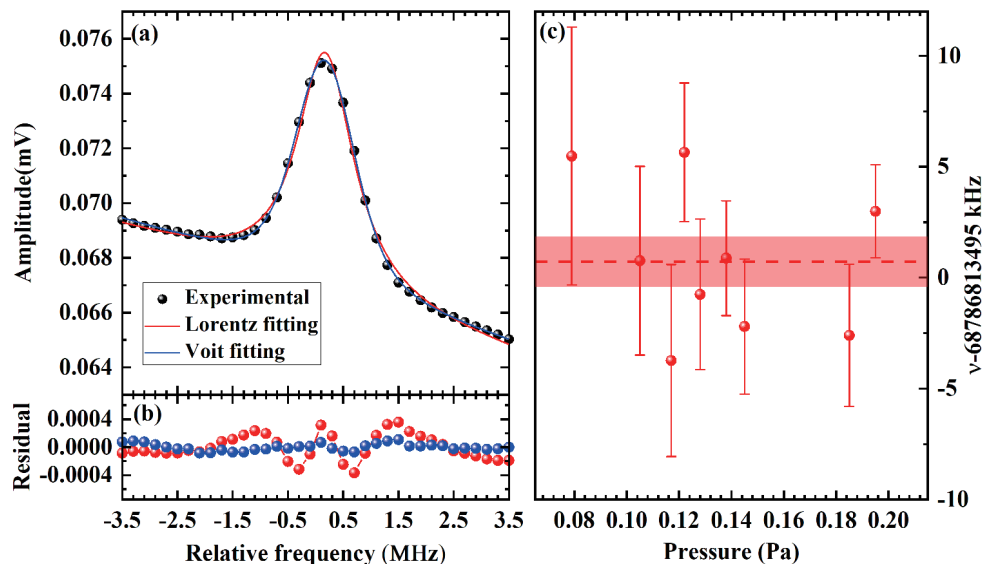


FIG. 3 The saturated absorption spectroscopy measurements of the R(14) (00011)-(00001) transition of $^{13}\text{CO}_2$. (a) An example of the saturated absorption spectrum. (b) Fitting residuals with Lorentzian (red) and Voigt (blue) line profile model. (c) Measurements under different sample pressures. The dashed line is the averaged transition frequency, and the red shadow shows the 1σ confidence band.

time of 40 s.

In order to demonstrate the accuracy of the MIR laser source, the saturated absorption of R(14) (00011)–(00001) transition of $^{13}\text{CO}_2$ is measured. The spectroscopy scan is accomplished by actively tuning the beat frequency between the signal lights of the OPO and the OFC while keeping the pump light locking at a single frequency point. The lamb dip, shown in FIG. 3(a), appears while scanning the laser where the spectroscopic background comes from the Doppler-limited absorption that we used for sample pressure calibration. The spectrum can be well-fitted with the Voigt profile, and the fitting residuals are shown in FIG. 3(b). The spectroscopic resolution or linewidth is 1.3 MHz, which is dominated by the transit-time broadening and the power broadening under the low sample pressure condition. The spectra were acquired at sample pressures ranging from 0.08 Pa to 0.2 Pa, and the center frequencies are shown in FIG. 3(c). Each datum in the figure represents the spectrum with an average of 100 scans, and the statistical uncertainty of the spectral center is less than 5 kHz. The excellent agreement among the data points indicates that there is no significant pressure-induced transition frequency shift within the uncertainty at such a low sample pressure, in good agreement with our previous study [33] in the CO molecule. The horizontal dashed line depicted in FIG. 3(c) represents the weighted mean value of line positions, and the red shadow indicates the 1σ confi-

dence band corresponding to the statistical uncertainty of 1.2 kHz.

Other contributions of the frequency uncertainty have been investigated. An uncertainty of less than 2 kHz is included due to the fitting model of the line profile, which is derived by comparing the fitted center frequency results with different line profile models. The laser frequency is determined by the comb mode frequency, the locking point monitored by the beat frequency between the pump/signal light and the comb, and the radio frequencies applied on AOM. The comb mode frequency uncertainty relies on the hydrogen maser and can be calculated to be less than 10 Hz for the MIR frequency. During the measurement, the beat frequency is monitored by a high-accurate frequency counter, which shows a frequency fluctuation below 1 kHz, as illustrated in FIG. 2(b). The radio frequency employed on the AOM, f_{AOM} , exhibits a fluctuation of less than 50 Hz, mainly due to the variation of the room temperature. Assuming the most probable speed of 330 m/s for the $^{13}\text{CO}_2$ molecule at 296 K, the frequency shift from the second-order Doppler effect is calculated to be 0.1 kHz with an uncertainty of about 40 Hz. In the experiment, the total laser power is 0.2 mW, and the AC-Stark shift is negligible for this transition. The potential misalignment angle between the pump and probe beams leads to a frequency uncertainty [35, 36]. In our experiment, the upper limit of the misalignment is estimated to be 0.78 mrad from the geometric config-

TABLE I Uncertainty budget of R(14) (00011)–(00001) transition of $^{13}\text{CO}_2$.

Effect	Correction/kHz	1σ /kHz
Statistic		1.2
Line profile asymmetry		<2
Comb mode frequency		<0.01
Laser locking		<1
AOM frequency		0.05
2nd order Doppler	0.1	0.04
Misalignment		29

Note: the total transition frequency R(14) (00011)–(00001) of CO_2 is 68786813496±29 kHz, while the reported value in Ref.[43] is 68786813426±87 kHz.

uration of the setup, and the resulting frequency uncertainty is 29 kHz. Note that the misalignment can be minimized by plenty of techniques, including the prism reflection method [37, 38], the cat's eye method [39], the interferometric method [40] and the active fiber-based retroreflector (AFR) method [41, 42].

The transition frequency uncertainty budget is presented in Table I. The transition frequency for line R(14) (00011)–(00001) is determined to be 68786813496 kHz, with an overall uncertainty of 29 kHz. The measured transition frequency agrees with the value of 68786813426±87 kHz [43], but the accuracy has been improved by a factor of three. The method of saturated absorption measurement can be applied to various molecules. For some molecules, such as CH_4 , the spectrum is spread over a range of hundreds of wavenumbers. We are developing a method to automatically scan the laser frequency and record the saturated absorption spectrum.

IV. CONCLUSION

We developed a narrow-linewidth continuous-wave MIR light source based on a laser-locked optical parametric oscillator. Both the OPO pump and signal lights were locked on the NIR OFC. The frequency accuracy of the MIR output (idler light) emitted from the system was checked by measuring the frequency stability of both the OPO pump and signal light simultaneously. The long-term frequency drift was determined to be less than 1 kHz. The frequency stabilized OPO system was applied to measure the saturated absorption spectroscopy of R(14) (00011)–(00001) in $^{13}\text{CO}_2$ at 4.3 μm . Doppler-free Lamb-dip signal was observed, and the transition frequency was determined with an accuracy

of 29 kHz. The demonstration proved that the frequency-stabilized MIR laser source can be used for precision spectroscopy measurements of molecules. The system provides an opportunity for some other applications, such as vibrational state-selected chemical dynamics [44, 45], and the optical detection of rare molecular isotopes like radioactive $^{14}\text{CO}_2$ [46, 47].

V. ACKNOWLEDGMENTS

This work was jointly supported by the National Natural Science Foundation of China (No.22241302, No.22373002, No.12393825, No.11974328), the Chinese Academy of Science (No.YSBR-055), and the Anhui Provincial Leading Talents Project.

- [1] M. S. Safronova, D. Budker, D. DeMille, D. F. J. Kimball, A. Derevianko, and C. W. Clark, *Rev. Mod. Phys.* **90**, 025008 (2018).
- [2] T. Steimle and W. Ubachs, *J. Mol. Spectrosc.* **300**, 1 (2014).
- [3] T. Rosenband, D. B. Hume, P. O. Schmidt, C. W. Chou, A. Brusch, L. Lorini, W. H. Oskay, R. E. Drullinger, T. M. Fortier, J. E. Stalnaker, S. A. Diddams, W. C. Swann, N. R. Newbury, W. M. Itano, D. J. Wineland, and J. C. Bergquist, *Science* **319**, 1808 (2008).
- [4] B. J. Bloom, T. L. Nicholson, J. R. Williams, S. L. Campbell, M. Bishof, X. Zhang, W. Zhang, S. L. Bromley, and J. Ye, *Nature* **506**, 71 (2014).
- [5] T. W. Hänsch, *Rev. Mod. Phys.* **78**, 1297 (2006).
- [6] C. W. Chou, D. B. Hume, T. Rosenband, and D. J. Wineland, *Science* **329**, 1630 (2010).
- [7] B. Spaun, P. B. Changala, D. Patterson, B. J. Bjork, O. H. Heckl, J. M. Doyle, and J. Ye, *Nature* **533**, 517 (2016).
- [8] A. Cingöz, D. C. Yost, T. K. Allison, A. Ruehl, M. E. Fermann, I. Hartl, and J. Ye, *Nature* **482**, 68 (2012).
- [9] L. G. Tao, A. W. Liu, K. Pachucki, J. Komasa, Y. R. Sun, J. Wang, and S. M. Hu, *Phys. Rev. Lett.* **120**, 153001 (2018).
- [10] J. Biesheuvel, J. P. Karr, L. Hilico, K. S. E. Eikema, W. Ubachs, and J. C. J. Koelemeij, *Nat. Commun.* **7**, 10385 (2016).
- [11] S. Patra, M. Germann, J. P. Karr, M. Haidar, L. Hilico, V. I. Korobov, F. M. J. Cozijn, K. S. E. Eikema, W. Ubachs, and J. C. J. Koelemeij, *Science* **369**, 1238 (2020).
- [12] E. R. Hudson, H. J. Lewandowski, B. C. Sawyer, and J. Ye, *Phys. Rev. Lett.* **96**, 143004 (2006).
- [13] A. Shelkownikov, R. J. Butcher, C. Chardonnet, and

- A. Amy-Klein, *Phys. Rev. Lett.* **100**, 150801 (2008).
- [14] W. Ubachs, J. Bagdonaite, E. J. Salumbides, M. T. Murphy, and L. Kaper, *Rev. Mod. Phys.* **88**, 021003 (2016).
- [15] C. Daussy, T. Marrel, A. Amy-Klein, C. T. Nguyen, C. J. Bordé, and C. Chardonnet, *Phys. Rev. Lett.* **83**, 1554 (1999).
- [16] E. J. Salumbides, J. C. J. Koelemeij, J. Komasa, K. Pachucki, K. S. E. Eikema, and W. Ubachs, *Phys. Rev. D* **87**, 112008 (2013).
- [17] M. Germann, S. Patra, J. P. Karr, L. Hilico, V. I. Korobov, E. J. Salumbides, K. S. E. Eikema, W. Ubachs, and J. C. J. Koelemeij, *Phys. Rev. Res.* **3**, L022028 (2021).
- [18] C. F. Cheng, Y. R. Sun, H. Pan, J. Wang, A. W. Liu, A. Campargue, and S. M. Hu, *Phys. Rev. A* **85**, 024501 (2012).
- [19] F. M. J. Cozijn, P. Dupré, E. J. Salumbides, K. S. E. Eikema, and W. Ubachs, *Phys. Rev. Lett.* **120**, 153002 (2018).
- [20] T. J. Kulp, S. E. Bisson, R. P. Bambha, T. A. Reichardt, U. B. Goers, K. W. Aniolek, D. A. V. Kliner, B. A. Richman, K. M. Armstrong, R. Sommers, R. Schmitt, P. E. Powers, O. Levi, T. Pinguet, M. Fejer, J. P. Koplrow, L. Goldberg, and T. G. Mcrae, *Appl. Phys. B* **75**, 317 (2002).
- [21] M. M. J. W. van Herpen, S. Li, S. E. Bisson, S. T. L. Hekkert, and F. J. M. Harren, *Appl. Phys. B* **75**, 329 (2002).
- [22] F. Müller, A. Popp, F. Kühnemann, and S. Schiller, *Opt. Express* **11**, 2820 (2003).
- [23] A. Clairon, B. Dahmani, A. Filimon, and J. Rutman, *IEEE Trans. Instrum. Meas.* **IM-34**, 265 (1985).
- [24] K. J. Siemsen, J. E. Bernard, A. A. Madej, and L. Marmet, *Appl. Phys. B* **72**, 567 (2001).
- [25] J. Faist, F. Capasso, D. L. Sivco, C. Sirtori, A. L. Hutchinson, and A. Y. Cho, *Science* **264**, 553 (1994).
- [26] M. Beck, D. Hofstetter, T. Aellen, J. Faist, U. Oesterle, M. Illegems, E. Gini, and H. Melchior, *Science* **295**, 301 (2001).
- [27] A. Gambetta, E. Vicentini, N. Coluccelli, Y. Wang, T. T. Fernandez, P. Maddaloni, P. De Natale, A. Castrillo, L. Gianfrani, P. Laporta, and G. Galzerano, *APL Photonics* **3**, 046103 (2018).
- [28] D. Mazzotti, P. Cancio, G. Giusfredi, P. De Natale, and M. Prevedelli, *Opt. Lett.* **30**, 997 (2005).
- [29] K. Takahata, T. Kobayashi, H. Sasada, Y. Nakajima, H. Inaba, and F. L. Hong, *Phys. Rev. A* **80**, 032518 (2009).
- [30] D. Chen, D. Hinkley, J. Pyo, J. Swenson, and R. Fields, *J. Opt. Soc. Am. B* **15**, 1693 (1998).
- [31] E. V. Kovalchuk, T. Schuldt, and A. Peters, *Opt. Lett.* **30**, 3141 (2005).
- [32] I. Ricciardi, E. De Tommasi, P. Maddaloni, S. Mosca, A. Rocco, J. J. Zondy, M. De Rosa, and P. De Natale, *Opt. Express* **20**, 9178 (2012).
- [33] J. Wang, Y. R. Sun, L. G. Tao, A. W. Liu, and S. M. Hu, *J. Chem. Phys.* **147**, 091103 (2017).
- [34] Z. T. Zhang, C. F. Cheng, Y. R. Sun, A. W. Liu, and S. M. Hu, *Opt. Express* **28**, 27600 (2020).
- [35] C. J. Bordé, J. L. Hall, C. V. Kunasz, and D. G. Hummer, *Phys. Rev. A* **14**, 236 (1976).
- [36] S. E. Park, H. S. Lee, T. Y. Kwon, and H. Cho, *Opt. Commun.* **192**, 49 (2001).
- [37] D. J. Berkeland, E. A. Hinds, and M. G. Boshier, *Phys. Rev. Lett.* **75**, 2470 (1995).
- [38] R. C. Brown, S. J. Wu, J. V. Porto, C. J. Sansonetti, C. E. Simien, S. M. Brewer, J. N. Tan, and J. D. Gillaspay, *Phys. Rev. A* **88**, 069902 (2013).
- [39] D. Shiner, R. Dixon, and P. Zhao, *Phys. Rev. Lett.* **72**, 1802 (1994).
- [40] S. Hannemann, E. J. Salumbides, and W. Ubachs, *Opt. Lett.* **32**, 1381 (2007).
- [41] A. Beyer, L. Maisenbacher, A. Matveev, R. Pohl, K. Khabarova, Y. Chang, A. Grinin, T. Lamour, T. Shi, D. C. Yost, T. Udem, T. W. Hänsch, and N. Kolachevsky, *Opt. Express* **24**, 17470 (2016).
- [42] V. Wirthl, L. Maisenbacher, J. Weitenberg, A. Hertlein, A. Grinin, A. Matveev, R. Pohl, T. W. Hänsch, and T. Udem, *Opt. Express* **29**, 7024 (2021).
- [43] B. M. Elliott, K. Sung, and C. E. Miller, *J. Mol. Spectrosc.* **312**, 78 (2015).
- [44] W. E. Perreault, N. Mukherjee, and R. N. Zare, *Nat. Chem.* **10**, 561 (2018).
- [45] W. E. Perreault, H. W. Zhou, N. Mukherjee, and R. N. Zare, *Phys. Rev. Lett.* **124**, 163202 (2020).
- [46] A. J. Fleisher, D. A. Long, Q. N. Liu, L. Gameson, and J. T. Hodges, *J. Phys. Chem. Lett.* **8**, 4550 (2017).
- [47] I. Galli, S. Bartalini, S. Borri, P. Cancio, D. Mazzotti, P. De Natale, and G. Giusfredi, *Phys. Rev. Lett.* **107**, 270802 (2011).